Geological Magazine

www.cambridge.org/geo

Carbon-isotope stratigraphy of the SPICE event (Upper Cambrian) in eastern Laurentia: implications for global correlation and a potential reference section

Karem Azmy

Department of Earth Sciences, Memorial University of Newfoundland, St John's, NL A1B 3X5, Canada

Original Article

Cite this article: Azmy K (2019) Carbon-isotope stratigraphy of the SPICE event (Upper Cambrian) in eastern Laurentia: implications for global correlation and a potential reference section. *Geological Magazine* **156**: 1311–1322. https://doi.org/10.1017/S0016756818000638

Received: 16 April 2018
Revised: 12 July 2018
Accepted: 22 August 2018
First published online: 30 October 2018

Keywords:
Furongian (Late Cambrian); SPICE event; high-resolution $\delta^{13}C$ chemostratigraphy; Laurentia; Martin Point (NL, Canada)

Author for correspondence:
Karem Azmy, Email: kazmy@mun.ca

Abstract

The $\delta^{13}C$ profile from the lower interval of the Martin Point section in western Newfoundland (Canada) spans the Upper Cambrian (uppermost Franconian – lowermost Trempealeauan). The investigated interval (~110 m) is a part of the Green Point Formation of the Cow Head Group and consists of the upper part of the Tucker Cove Member (topmost part of the Shallow Bay Formation) and the lowermost part of the Martin Point Member (bottom of the Green Point Formation). It is formed of rhythmites of marine carbonates alternating with shales and minor conglomeratic interbeds. Multiscreening petrographic and geochemical techniques have been utilized to evaluate the preservation of the investigated lime mudstones. The $\delta^{13}C$ and $\delta^{18}O$ values of the sampled micrites (−4.8 ‰ to +1.0 ‰ VPDB and −8.2 ‰ to −5.3 ‰ VPDB, respectively) have insignificant correlation ($R^2 = 0.01$), as similarly do the $\delta^{13}C$ values with their Sr counterparts ($R^2 = 0.07$), which supports the preservation of at least near-primary $\delta^{13}C$ signatures that can be utilized to construct a reliable high-resolution carbon-isotope profile for global correlations. The $\delta^{13}C$ profile exhibits two main negative excursions: a lower excursion (~4 ‰) that reaches its maximum at the bottom of the section and an upper narrow excursion (~6 ‰) immediately above the boundary of the Tucker Cove/Martin Point members (Shallow Bay Formation – Green Point Formation boundary). The lower excursion may be correlated with the global SPICE event, whereas the upper excursion may match with a post-SPICE event that has been also recognized in profiles of equivalent sections on different palaeocontinents.

1. Introduction

Primary stable isotope signatures retained in preserved carbonates (e.g. Veizer *et al.* 1999) have been found to be a potential tool for chemostratigraphic correlations, particularly for sections with poor biostratigraphic resolution. Primary/near-primary $\delta^{13}C$ variations, associated with eustatic sealevel changes, allow the construction of reliable profiles for correlating sedimentary sequences of different depositional settings within the same basin (e.g. Miller *et al.* 2011, 2014; Azomani *et al.* 2013) and from different palaeocontinents (e.g. Jing *et al.* 2008; Azmy *et al.* 2010; Miller *et al.* 2011, 2014). The eustatic changes along the eastern Laurentian passive margin during latest Cambrian time influenced the redox conditions of the depositional environment (e.g. Azmy *et al.* 2015; Azmy, 2018) and, accordingly, primary organic productivity along with the C-isotope compositions of marine carbonates (e.g. Landing, 2007, 2012a; Landing *et al.* 2010; Miller *et al.* 2011, 2014; Terfelt *et al.* 2014; Azmy *et al.* 2014, 2015).

The main objectives of the current study are to evaluate the petrographic and geochemical preservation of the carbonates of the lower Martin Point section (western Newfoundland, Canada) that spans the Upper Cambrian (Furongian) and to reconstruct a reliable primary C-isotope profile that allows the recognition of the stratigraphic levels of the SPICE (Steptoean Positive Carbon Isotope Excursion) and the post-SPICE (below the HERB event: Hellnmaria–Red Tops Boundary, also called the TOCE: Top Of Cambrian Excursion) events. This will also enhance the global correlation of the Upper Cambrian on Laurentia and beyond.

2. Geologic setting

Palaeozoic sedimentary rocks of western Newfoundland in Canada (Fig. 1) were deposited on the eastern Laurentian margin. The Laurentian plate developed by active rifting around 570–550 Ma (e.g. Cawood *et al.* 2001; Hibbard *et al.* 2007), and a pre-platform shelf formed and was eventually covered by clastic sediments (James *et al.* 1989). A major transgression flooded the Laurentian platform margin and resulted in the accumulation of thick carbonate deposits (Wilson *et al.* 1992; Landing, 2007, 2012a; Lavoie *et al.* 2012).

CAMBRIDGE UNIVERSITY PRESS

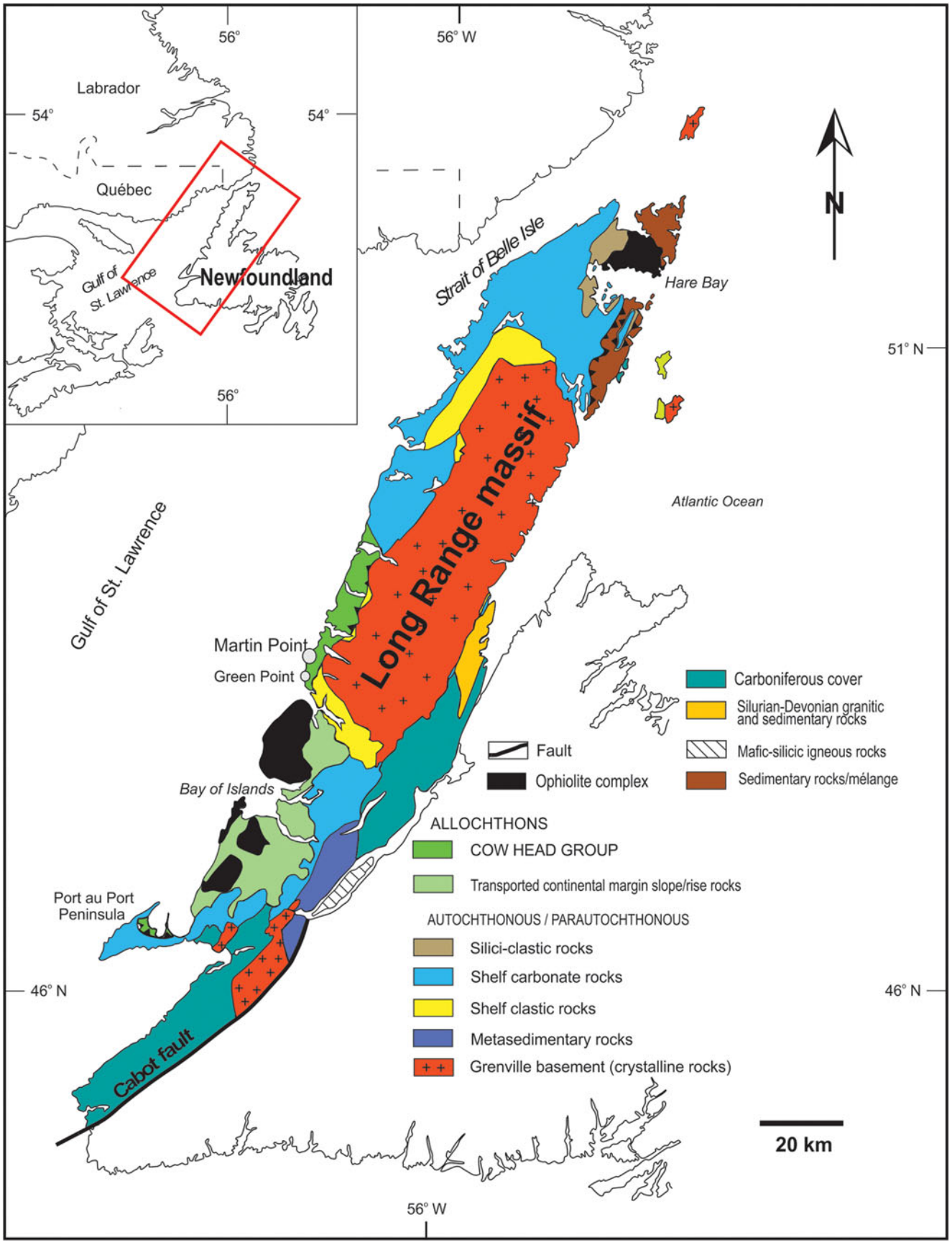

Fig. 1. (Colour online) Map of the study area showing the surface geology and location of the Martin Point section (49° 40′ 51″ N, 57° 57′ 36″ W) in western Newfoundland, Canada (modified from James & Stevens, 1986; Cooper *et al.* 2001).

https://doi.org/10.1017/S0016756818000638 Published online by Cambridge University Press

3. Stratigraphy

3.a. Lithostratigraphy

The lithostratigraphy of the investigated interval of the lower Martin Point section spans the Upper Cambrian, particularly the uppermost part of the Shallow Bay Formation (upper Tuckers Cove Member) and the lowermost part of the Green Point Formation (lower Martin Point Member) of the Cow Head Group (Fig. 2). It has been studied and discussed in detail by James & Stevens (1986), and it will therefore only be summarized here. The section consists of dark grey to black fissile shale alternating with thin (~1 cm thick) interbeds of ribbon limestone rhythmites. Those rhythmites were precipitated *in situ* slowly in a calm environment as primary carbonates either directly from seawater or possibly by biomediation, which is indicated by lamination (e.g. Della Porta *et al.* 2003; Bahamonde *et al.* 2007; Bartley *et al.* 2015). Siltstone interbeds (up to 1 cm thick) may co-occur with shale but are not abundant, and the limestone interbeds (rhythmites) vary from isolated and thin to up to 20 cm thick. Carbonate conglomerate/breccia beds may occur and contain clasts (up to 25 cm) of shallow-water carbonates that were transported into deep-water facies along the slope of the Laurentian margin (James & Stevens, 1986).

3.b. Biostratigraphy

The age of the investigated interval covers the uppermost Franconian and the lowermost Trempealeauan, which is well below the upper boundary of the so-called *Lotagnostus americanus* trilobite Zone that has been proposed for the base of the uppermost Cambrian Stage (Cooper *et al.* 2001), although Landing *et al.* (2010, 2011) and Westrop *et al.* (2011) limit *L. americanus* to topotype material in Quebec and do not agree that the lowest occurrence of this agnostoid arthropod is appropriate for defining a global chronostratigraphic unit. However, the lower boundary of the zone seems to be far down below the exposed section (Cooper *et al.* 2001). The conodont biozonation documented for the studied section at Martin Point (Fig. 2) spans approximately the lower part of the *Proconodontus muelleri* Zone and reaches down to the *Proconodontus posterocostatus* Zone on the global conodont biozonation scheme including that of N. America (James & Stevens, 1986; Barnes, 1988; Miller *et al.* 2011; Li *et al.* 2017). The *P. muelleri* and *P. posterocostatus* zones have been documented below the *Eoconodontus notchpeakensis* Zone in the Lawson Cove and Sneakover Pass sections of Utah, USA (Miller *et al.* 2011), where the base of the *notchpeakensis* Zone is marked by the distinct HERB $\delta^{13}C$ excursion (Miller *et al.* 2011; Li *et al.* 2017; Azmy, 2018). The HERB $\delta^{13}C$ excursion has been documented in the GSSP section of Green Point (e.g. Miller *et al.* 2011) and that of the Martin Point section (Azmy, 2018) at a stratigraphic level well above the currently investigated interval. However, the *P. muelleri* and *P. posterocostatus* zones have not been documented yet in the Martin Point section but, based on the global biozonation scheme, are expected to be at a stratigraphic level correlated with that of the currently studied interval (Fig. 2).

4. Material and methodology

Fifty closely spaced samples (Appendix Table A1; Fig. 2) were collected from the lower part of the Martin Point section (49° 40′ 51″ N, 57° 57′ 36″ W; James & Stevens, 1986; Cooper *et al.* 2001), western Newfoundland (Fig. 1). Samples were taken from laminated lime mudstone interbeds to avoid allochthonous clasts. Thin-sections of samples were petrographically examined with a polarizing microscope and stained with Alizarin Red–S and potassium ferricyanide solutions (Dickson, 1966). Cathodoluminescence (CL) observations were performed using a Technosyn 8200 MKII cold cathode instrument operated at 8 kV accelerating voltage and 0.7 mA current.

A mirror-image slab of each thin-section was also prepared and polished for microsampling. The polished slabs were washed with deionized water and dried overnight at 50 °C prior to isolating the finest grained lime mudstone free of secondary cements and other contaminants. Owing to the possible heterogeneity in geochemical compositions of texturally distinct carbonate phases in whole-rock samples, and in order to avoid silicate inclusions and secondary carbonate cements and veins, microsamples were drilled from the finest grained micritic material under a binocular microscope. Approximately 10 mg of carbonate was microsampled from the cleaned slabs using a low-speed microdrill under a binocular microscope.

For C- and O-isotope analyses, about 220 μg of powder sample was reacted in an inert atmosphere with ultrapure concentrated (100 %) orthophosphoric acid at 70 °C in a ThermoFinnigan GasBench II. The liberated CO_2 was automatically delivered to a ThermoFinnigan DELTA V plus isotope ratio mass spectrometer in a stream of helium, where the gas was ionized and measured for isotope ratios. Uncertainties of better than 0.1 ‰ (2σ) for the analyses were determined by repeated measurements of NBS-19 ($\delta^{18}O = -2.20$ ‰ and $\delta^{13}C = +1.95$ ‰ v. VPDB (Vienna Pee Dee Belemnite)) and L-SVECS ($\delta^{18}O = -26.64$ ‰ and $\delta^{13}C = -46.48$ ‰ v. VPDB).

For elemental analyses, a subset of sample powder (~10 mg each) was digested in 2 % (v/v) HNO_3 and analysed for major and trace elements using an Elan DRC II inductively coupled plasma mass spectrometer (ICP-MS) (Perkin Elmer SCIEX). The relative uncertainties of these measurements are less than 5 %, and results are normalized to a 100 % carbonate basis (e.g. Azmy *et al.* 2014).

5. Results

Petrographic examinations indicate that the currently investigated carbonates of the lower Martin Point section are dominantly lime mudstones, which have retained at least their near-micritic texture and appear dull under cathodoluminescence (Fig. 3a,b).

The geochemical characteristics of those carbonates are tabulated in Appendix Table A1 and the statistics of the results are summarized in Table 1. Their mean Sr content (308 ± 224 ppm) is very comparable to that of the overlying section of carbonates that records the HERB event (Table 1; Azmy, 2018), although their Mn content (291 ± 154 ppm) is lower (Table 1). The Mn and Fe contents of the investigated carbonates show insignificant correlations with their Sr counterparts ($R^2 = 0.1$ and 0.06, respectively).

The Sr and Al values exhibit insignificant correlations with their $\delta^{13}C$ ($R^2 = 0.07$ and 0.003, respectively; Fig. 4a,b) and $\delta^{18}O$ counterparts ($R^2 = 0.02$ and 0.01, respectively; Appendix Table A1).

The mean $\delta^{13}C$ and $\delta^{18}O$ values of the investigated carbonates (−1.0 ± 1.2 and −7.4 ± 0.5 ‰ VPDB, respectively; Table 1) fall mainly within the documented range of Upper Cambrian well-preserved marine carbonates (Fig. 4c; Veizer *et al.* 1999) and are comparable to their counterparts in the overlying section spanning the HERB event (Table 1; Azmy, 2018).

6. Discussion

The C-isotope composition of marine carbonates ($\delta^{13}C_{carb}$) may reflect the influence of depositional environment and/or

https://doi.org/10.1017/S0016756818000638 Published online by Cambridge University Press

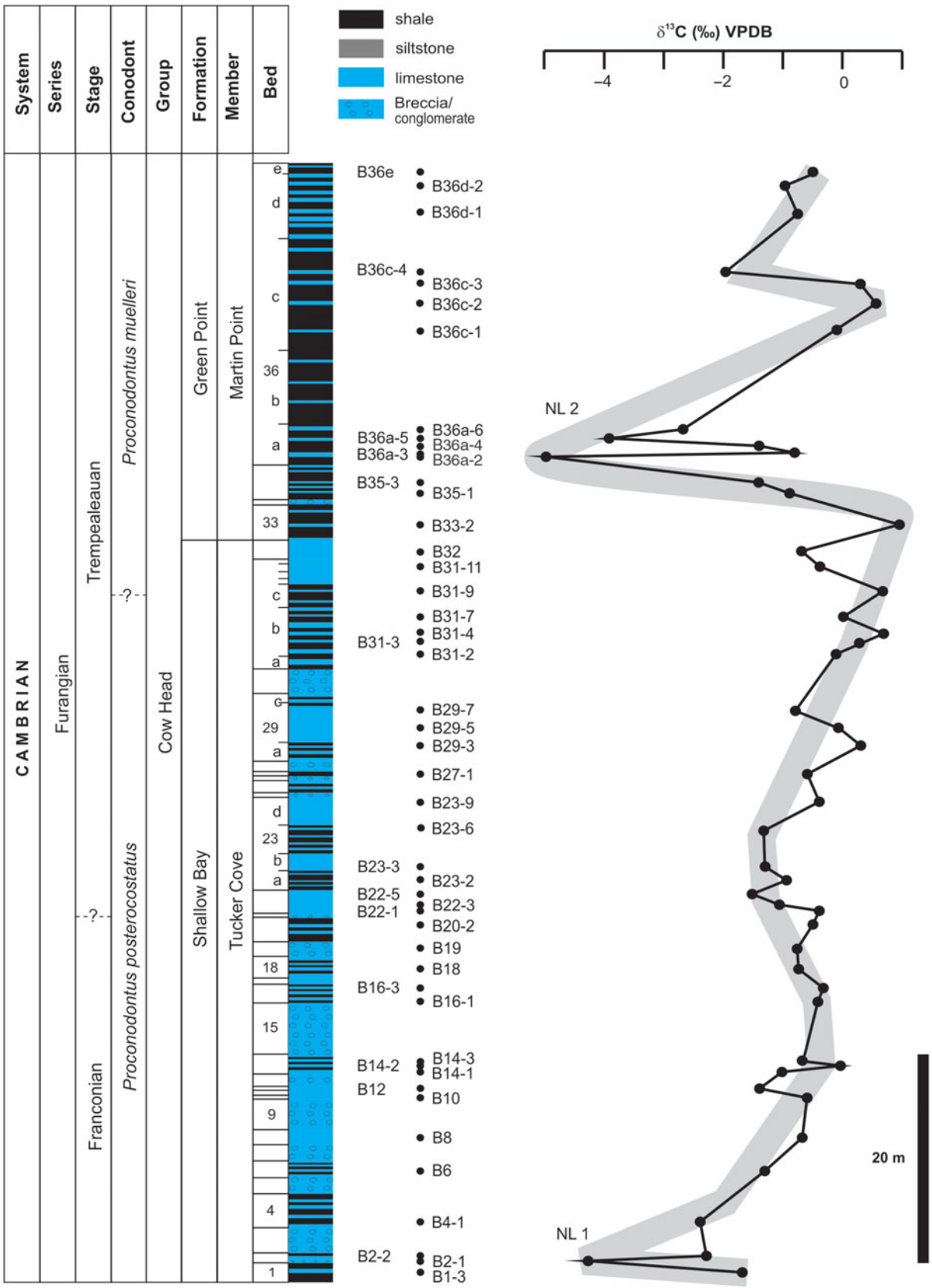

Fig. 2. (Colour online) Stratigraphic framework of the investigated lower Martin Point section in western Newfoundland, Canada (James & Stevens, 1986) showing bed number and detailed measured positions of investigated samples. The *P. muelleri* and *P. posterocostatus* zones have not been documented yet in the Martin Point section but are based on the global scheme (e.g. Li *et al.* 2017) and also on that suggested for the Cow Head Group and North America (Barnes, 1988; Miller *et al.* 2011). The grey line highlights the main changes in the $\delta^{13}C$ profile of the investigated carbonates.

https://doi.org/10.1017/S0016756818000638 Published online by Cambridge University Press

Table 1. Summary of statistics of isotopic and trace element geochemical compositions of the investigated Upper Cambrian carbonates of the lower Martin Point section

	$CaCO_3$ %	$MgCO_3$ %	Mn (ppm)	Sr (ppm)	$\delta^{13}C$ (‰ VPDB)	$\delta^{18}O$ (‰ VPDB)
Lower Martin Point Section (current study)						
n	32	32	30	32	50	50
average	97.3	2.7	291	308	−1.0	−7.4
stdev	5.2	5.2	154	224	1.2	0.5
max	99.4	29.8	802	1294	1.0	−5.3
min	70.2	0.6	91	73	−4.8	−8.2
Upper Martin Point section (HERB event; Azmy, 2018)						
n	25	25	25	25	63	63
average	98.4	1.6	360	324	−0.5	−7.1
stdev	0.7	0.7	160	192	0.8	0.3
max	99.0	3.7	649	980	1.0	−6.4
min	96.3	1.0	142	152	−2.1	−7.8

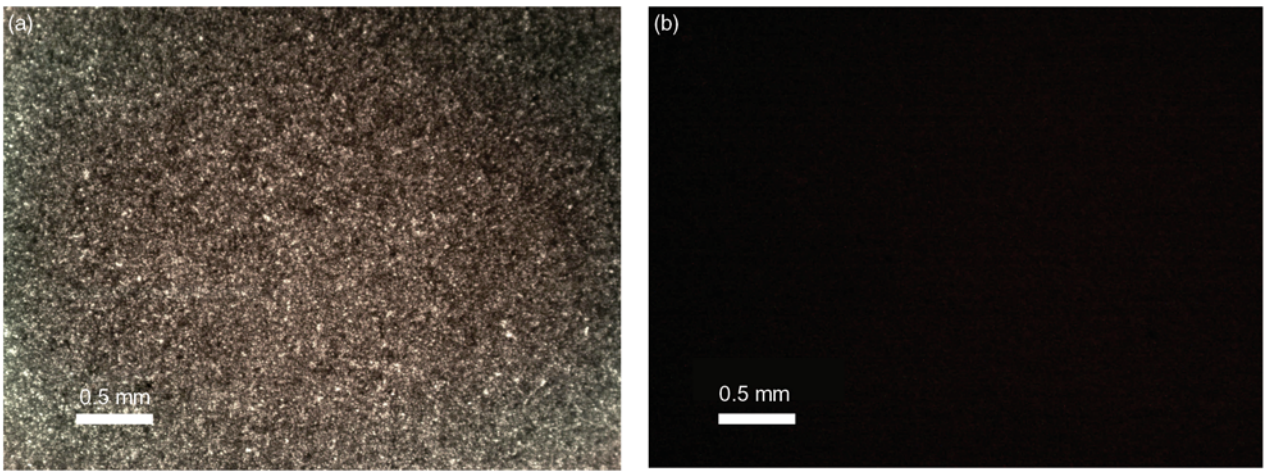

Fig. 3. (Colour online) Photomicrographs of the investigated carbonates showing, (a) micritic lime mudstones (Sample B31-1) and (b) CL image of (a).

diagenetic conditions, and C-isotope stratigraphy has to therefore be based on the primary $\delta^{13}C_{carb}$ signatures (e.g. Veizer *et al.* 1999; Azmy, 2018). Although ancient carbonates, such as those from the Palaeozoic Era, are almost impossible to be retained entirely unaffected by diagenetic fluids during their burial history, their alteration is at times so limited that they retain their near-primary geochemical signatures, particularly at low water/rock interaction ratios. Thus, the evaluation of the degree of sample preservation and the retained (primary or near-primary) isotopic and elemental geochemical signatures is the solid foundation for the reconstruction of $\delta^{13}C$ profiles that can be utilized for reliable high-resolution global chemostratigraphic correlations.

6.a. Influence of diagenesis

Multiscreening techniques (petrographic and geochemical) have been utilized to evaluate the preservation of the studied samples. The investigated carbonates of the Upper Cambrian Martin Point section are dominated by lime mudstones that exhibit insignificant recrystallization (Fig. 3). They retained their micritic to near-micritic grain size and sedimentary fabrics, thus reflecting a high degree of petrographic preservation (e.g. Azmy, 2018), which is also supported by their non-luminescent images under the cathodoluminscope (Fig. 3a,b). Luminescence in carbonates is mainly activated by high concentrations of Mn but quenched by high concentrations of Fe (Machel & Burton, 1991). Dull luminescence, in many cases, indicates relative preservation of primary geochemical signatures (e.g. Azmy, 2018), but diagenetic carbonates, such as late-burial cements, may still appear dull to non-luminescent owing to their high Fe contents (Rush & Chafetz, 1990). This may suggest that cathodoluminescence has to be taken with caution and complemented by additional screening tests (Brand *et al.* 2011). Alteration of carbonates is associated with depletion in Sr contents and $\delta^{18}O$ values but enrichment in Mn and Fe (Veizer, 1983). The investigated carbonates are believed to have been deposited in slope settings (James & Stevens, 1986), likely under less oxic (dysoxic) conditions (e.g. Azmy, 2018), where seawater is expected to be at least slightly more enriched in Mn than shallow water. Earlier studies have documented microbial lime mudstone in Palaeozoic slope

https://doi.org/10.1017/S0016756818000638 Published online by Cambridge University Press

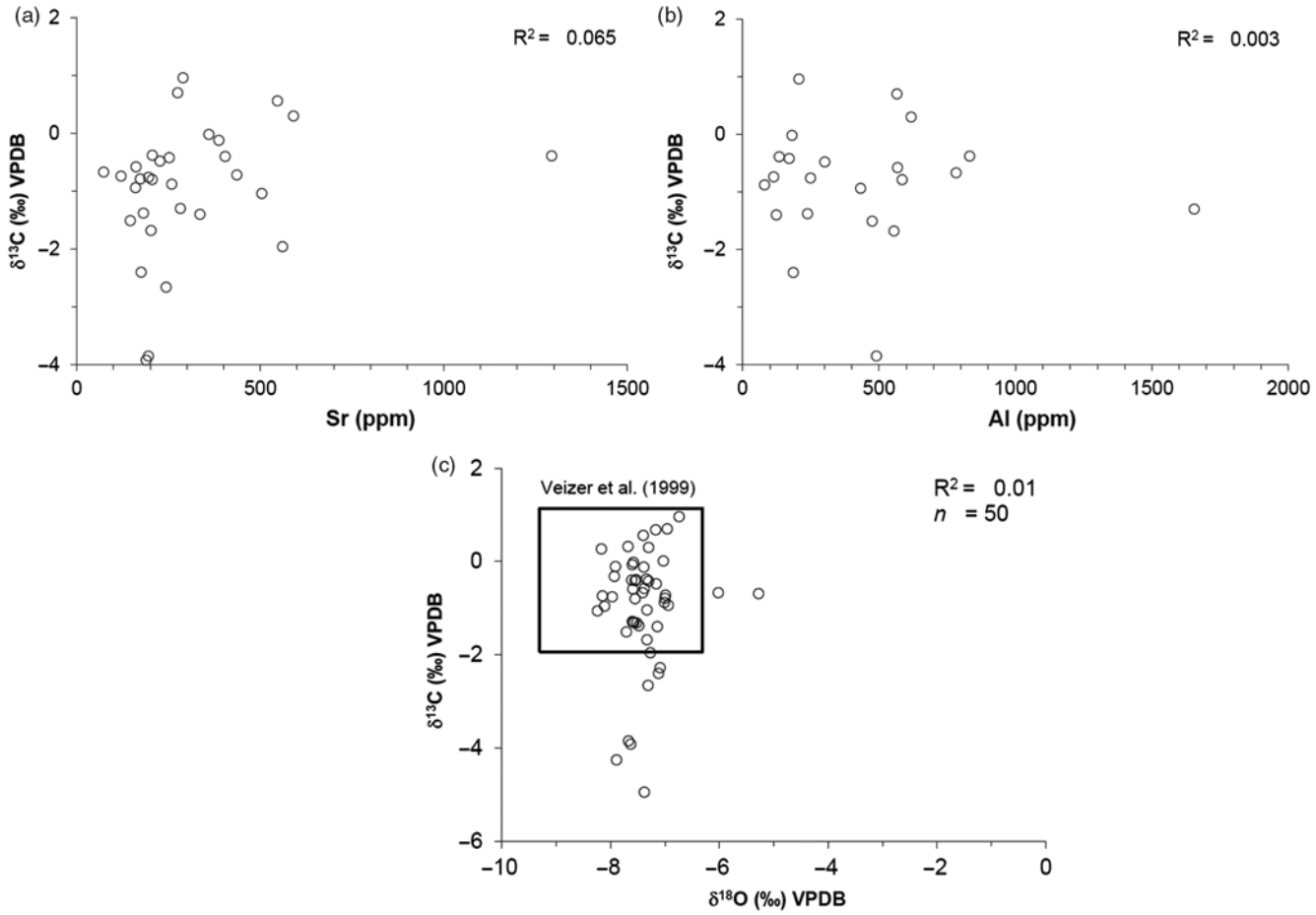

Fig. 4. Scatter diagrams showing correlations of (a) Sr (b) Al and (c) $\delta^{18}O$ with $\delta^{13}C$ for the micritic lime mudstones from the lower Martin Point section. The rectangle in (c) marks the composition of best-preserved Upper Cambrian carbonates (Veizer *et al.* 1999).

carbonates at depths down to 300 m (Della Porta *et al.* 2003; Bahamonde *et al.* 2007; Bartley *et al.* 2015). Thus, the lime mudstones of the current investigation had contributions from *in situ* carbonates that were deposited through microbial mediation and are expected to be slightly enriched in Mn relative to those of shallow-water settings (≤ 100 ppm; Veizer, 1983). Therefore, the enriched Mn contents of the Martin Point lime mudstones (291 ± 154 ppm; Table 1) are likely related to deposition in Mn-rich dysoxic waters (e.g. Azmy, 2018) rather than diagenetic alteration. Similarly, Fe is a redox proxy and is expected to be enriched in the investigated slope carbonates (1685 ± 1741 ppm; Appendix Table A1). Both the Mn and Fe contents are insignificantly correlated with their Sr counterparts (R^2 = 0.1 and 0.06, respectively), which argues against significant diagenetic alteration.

This is also consistent with the high Sr contents (up to 1294 ppm; Table 1; Appendix Table A1) and poor correlation of the Sr and Al values with their $\delta^{13}C$ counterparts (R^2 = 0.065 and 0.003; Fig. 4a,b), and with the clean, non-argillaceous lime mudstone interbeds where carbonate clasts are restricted only to the conglomeratic interbeds (Fig. 2) that occur occasionally (cf. James & Stevens, 1986; Coniglio & James, 1990; Li *et al.* 2006). The occurrence of shale interbeds would certainly lead to diagenetic fluids enriched in Al and consistent enrichment of Al in altered carbonates with progressive diagenesis. In addition, the poor correlation of the Sr and Mn contents with their $\delta^{18}O$ counterparts (R^2 = 0.02 and 0.03, respectively; Appendix Table A1) suggests that the alteration was likely restricted under a low water/rock interaction ratio of closed to semi-closed conditions (e.g. Azmy, 2018), which also explains the occurrence of the isotopic compositions of the investigated carbonates within the range of that documented for the best-preserved marine carbonates of the same age (Fig. 4c; Veizer *et al.* 1999).

Generally speaking, the preservation of primary/near-primary $\delta^{13}C$ signatures of carbonates is to some extent highly probable because the diagenetic fluids, in many cases, do not contain significant enough concentrations of CO_2 to reset the C-isotope composition unless high water/rock interaction ratios are achieved, which is associated with significant recrystallization and increase in crystal size (aggrading neomorphism). However, this is not the case in the currently investigated Martin Point lime mudstones, which retain micritc to near-micritic grain size (e.g. Azmy, 2018; Fig. 3a).

Recrystallization of carbonates during diagenesis may result in the alteration of their organic matter contents and the depletion of the primary $\delta^{13}C$ signatures of the carbonates. The micritic grain size of the investigated lime mudstones argues against significant recrystallization and organic remineralization. Also, this agrees with the very poor correlation of the Al values with those of $\delta^{13}C$ (R^2 = 0.003; Fig. 4b), which reflects the insignificant input of organic matter from terrestrial sources but mainly from marine sources.

https://doi.org/10.1017/S0016756818000638 Published online by Cambridge University Press

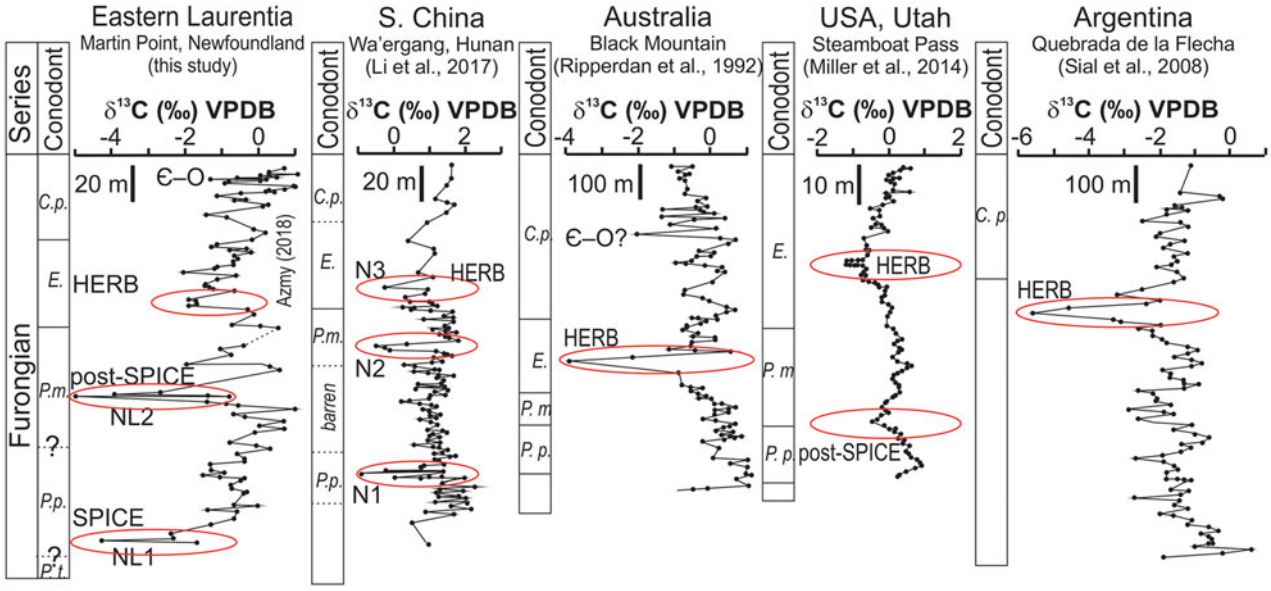

Fig. 5. (Colour online) Global C-isotope chemostratigraphic correlations of the SPICE event (late Cambrian) documented in comprehensive sections from basins on different palaeocontinents (modified from Barnes, 1988; Miller *et al.* 2011; Li *et al.* 2017). These sections may span up to the Cambrian–Ordovician boundary. Abbreviations of conodont biozones: *C.p.* – *Cordylodus proavus*; *E.* – *Eoconodontus*; *P.m.* – *Proconodontus muelleri*; *P.p.* – *Proconodontus posterocostatus*; *P.t.* – *Proconodontus tenuiserratus*. The peaks of the C-isotope excursions are marked.

In summary, the petrographic and geochemical preservation of the investigated carbonates supports the preservation of at least near-primary $\delta^{13}C$ compositions and suggests that their variations reflect the response to primary depositional conditions and can, therefore, be reliably utilized for high-resolution global chemostratigraphic correlations.

6.b. Carbon-isotope stratigraphy

The eustatic sealevel changes during Late Cambrian time (e.g. James & Stevens, 1986; Cooper *et al.* 2001; Landing, 2007, 2012a,b; Landing *et al.* 2010, 2011) influenced the abundance of biota and their productivity in oceans, which also resulted in changes in the global ocean water chemistry (e.g. Veizer *et al.* 1999; Li *et al.* 2017; Azmy, 2018) and the C-isotope composition of marine carbonates that recorded distinct negative $\delta^{13}C$ excursions (e.g. Jing *et al.* 2008; Sial *et al.* 2008; Terfelt *et al.* 2014; Miller *et al.* 2015; Li *et al.* 2017) due to the associated changes in redox conditions. Similar $\delta^{13}C$ excursions, caused by variations in primary productivity or organic preservation, have been documented in marine environment throughout the Earth's history (e.g. Veizer *et al.* 1999; Halverson *et al.* 2005).

The $\delta^{13}C$ profile of the currently investigated interval (Fig. 2) is recorded in the lower part of the exposed section at Martin Point, which spans the Upper Cambrian and has no documented sedimentary hiatuses (cf. James & Stevens, 1986; Cooper *et al.* 2001). It shows a lower C-isotope excursion of ~4 ‰ that peaks at the bottom of the section and an upper excursion of ~6 ‰ that peaks at Bed 36a (Fig. 2). Other excursions were documented in the C-isotope profile of the overlying carbonates at the Martin Point section and are believed to be correlated with the HERB (TOCE) and Cambrian–Ordovician (Є–O) boundary (Fig. 5; Azmy *et al.* 2014, 2015; Azmy, 2018), which is consistent with the established bio- (Miller *et al.* 2011) and lithostratigraphic (James & Stevens, 1986; Miller *et al.* 2011) correlations between the GSSP section at Green Point and its currently studied counterpart at Martin Point.

Based on the established global conodont biostratigraphic schemes of correlation for the Upper Cambrian (Barnes, 1988; Lazarenko *et al.* 2011; Miller *et al.* 2011; Peng *et al.* 2012), the global $\delta^{13}C$ profile of the Upper Cambrian (Li *et al.* 2017) generally shows a lowermost excursion called the SPICE event that correlates with the *Proconodontus posterocostatus* Zone, a distinct post-SPICE excursion that correlates with *Proconodontus muelleri* Zone, an upper excursion called HERB that correlates with the lower *Eoconodontus notchpeakensis* Zone and an uppermost excursion that correlates with the Є–O boundary (Fig. 5).

The global correlation of the HERB and Є–O boundary $\delta^{13}C$ excursions of the Martin Point succession have been discussed in detail by Azmy *et al.* (2014, 2015) and Azmy (2018), where they were documented in the upper part of the section (Fig. 5), but the current investigation focuses on the global correlation of the SPICE and post-SPICE $\delta^{13}C$ excursions from the lower part of the same section. The $\delta^{13}C$ profile of the Martin Point section shows a distinct excursion of ~6‰ (NL2) below the HERB event (Figs 2,5; Azmy, 2018) at a level possibly within the *Proconodontus muelleri* Zone, which is followed by a lower counterpart (NL1) of ~4 ‰ (Figs 2,5). Unfortunately, no conodont biozonation scheme has yet been reported below the level of the *P. muelleri* – *E. notchpeakensis* boundary in the Martin Point section (Fig. 5). However, accepting that the *P. muelleri* and the underlying *P. posterocostatus* zones are implied by the global scheme to occur immediately below the *E. notchpeakensis* Zone, NL2 may be correlated with the *P. muelleri* Zone since it occurs directly below the HERB (TOCE) excursion, which is correlated with the base of the *E. notchpeakensis* Zone (Azmy, 2018; Fig. 5). Thus, NL2 could be correlated with the global post-SPICE event (Fig. 5; N2 excursion in S. China; Li *et al.* 2006). NL1 is well below NL2 and may therefore be assigned to the *P. posterocostatus* Zone, but the exact position of NL1 within the *P. posterocostatus* Zone is not yet known since no detailed conodont biozonation has been documented below the upper boundary of the *P. muelleri* Zone in the Martin Point section. Further biostratigraphic studies will certainly refine the conodont biozonation scheme in the Martin Point section, and the currently proposed

https://doi.org/10.1017/S0016756818000638 Published online by Cambridge University Press

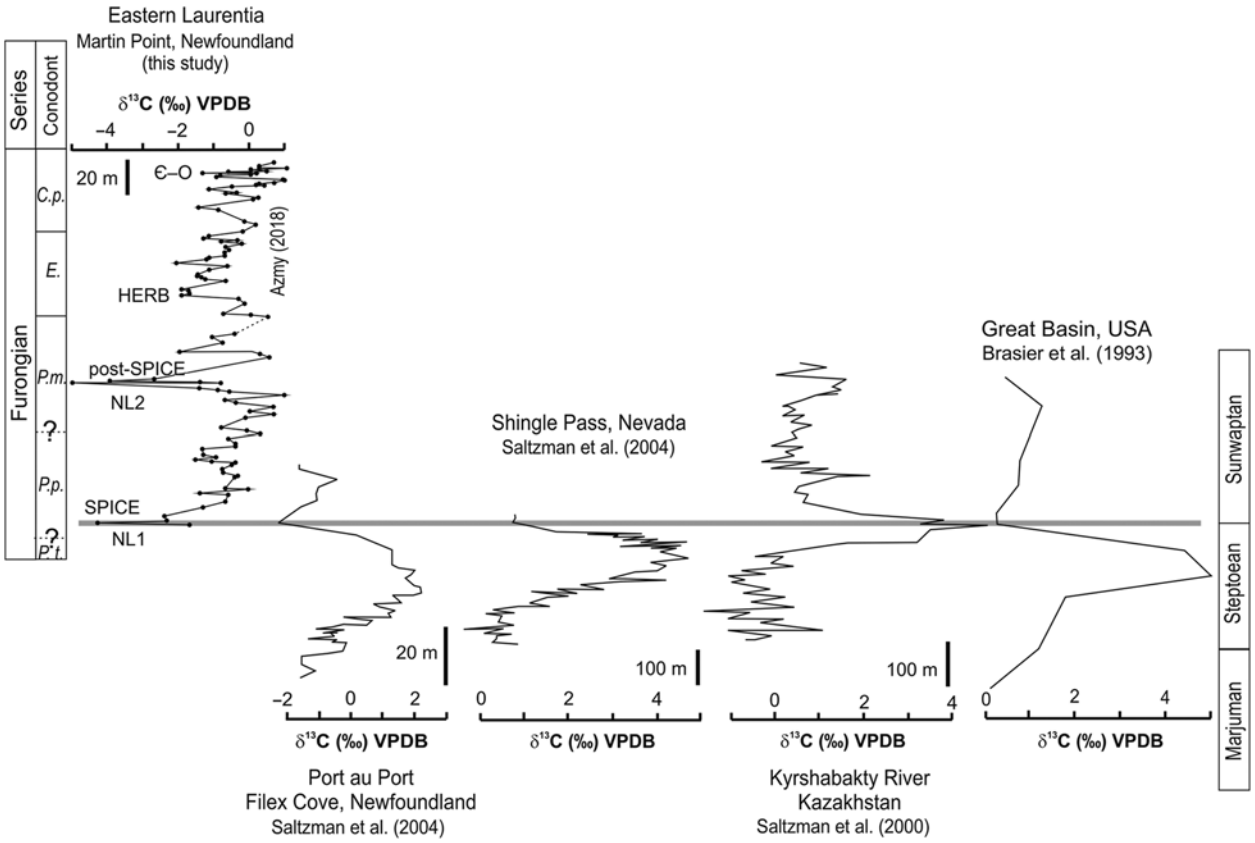

Fig. 6. Correlation of isolated positive SPICE $\delta^{13}C$ excursions that were documented in some earlier studies from basins on different palaeocontinents. These sections did not span time intervals younger than that of the SPICE. The grey line marks the suggested possible fit relative to the C-isotope profile of the Martin Point section and also the base of the *Irvingella* trilobite Zone (cf. Fan *et al.* 2011). Abbreviations of conodont zones as in Figure 5.

$\delta^{13}C$ chemostratigraphic correlations have to therefore be taken with caution.

Similar successive and comparable negative excursions, with comparable or different magnitude, have been documented for equivalent sections of shallow-water settings in the USA (Steamboat Pass section of Utah; Miller *et al.* 2015), Argentina (Buggisch *et al.* 2003; Sial *et al.* 2008, 2013), S. China (Wa'ergang, Hunan; Li *et al.* 2017) and Australia (Black Mountain; Ripperdan *et al.* 1992). The conodont biozonation scheme of the Upper Cambrian (Furongian) in Argentina starts with the *Cordylodus proavus* Zone at the end of the HERB event, but no record is known yet for the older interval (Miller *et al.* 2011). The lack of a conodont biozonation record below the *Cordylodus proavus* Zone (Fig. 5) in the Argentina section (cf. Sial *et al.* 2008; Miller *et al.* 2011; Terfelt *et al.* 2014) results in the correlation of its negative $\delta^{13}C$ excursions being based mainly on the assumption of a lack of significant unconformity surfaces, the relative stratigraphic levels of the excursions (Fig. 5) and their occurrence together within a single trilobite zone (*Saukia* Zone) that spans a major interval of the Furongian up to the end of the *Eoconodontus* conodont Zone Landing *et al.* 2010, 2011; Miller *et al.* 2011). The amplitudes of the correlated $\delta^{13}C$ excursions across the globe may vary, likely owing to differences in the local palaeo-oceanographic conditions such as depth and organic primary productivity.

The big advantage of the investigated Martin Point section is that it retains the primary full $\delta^{13}C$ record that spans from the excursion of the lowermost SPICE event (current study) to the uppermost excursion of the Є–O boundary, which are not all recorded together in other individual equivalent sections.

The SPICE event has been marked, in some earlier studies of carbonate sections from basins on different palaeocontinents, by an isolated individual positive $\delta^{13}C$ shift (e.g. Brasier, 1993; Saltzman *et al.* 2000, 2004; Glumac & Mutti, 2007; Hurtgen *et al.* 2009; Fan *et al.* 2011; Gill *et al.* 2011; Schmid, 2011; Woods *et al.* 2011; Dahl *et al.* 2014) that was globally correlated based on changes in trilobite biozones (Fig. 6). However, the short time interval spanned by those sections, relative to that of the Martin Point section, and the lack of details of the immediately overlying younger $\delta^{13}C$ variations make it hard to reconcile their profiles with that of the Martin Point section. The best fit, however, at this stage, for those positive excursions could be by placing their uppermost negative peaks (inflecting from the positive excursion) at the stratigraphic level of the peak of the negative excursion of the SPICE event on the Martin Point profile (Fig. 6). The suggested level generally matches the base of the *Irvingella* trilobite Zone (Saltzman *et al.* 2000), except for in very few locations such as Kazakhstan (Fig. 6; Saltzman *et al.* 2000; Fan *et al.* 2011).

The Martin Point section seems to be a complete and continuous interval, consisting of rhythmites with petrographically preserved lime mudstone interbeds (e.g. Azmy, 2018) that retain near-primary geochemical signatures, and has no documented sedimentary hiatuses (James & Stevens, 1986). It spans the entire interval of the Upper Cambrian until the Є–O boundary, and its C-isotope profile exhibits a complete set of the global $\delta^{13}C$

https://doi.org/10.1017/S0016756818000638 Published online by Cambridge University Press

excursions documented for that time interval from the SPICE event to the Є–O boundary, which suggests that the section can be a potential alternative reference for the entire Upper Cambrian on Laurentia.

7. Conclusions

(a) The petrographic and geochemical examinations support the preservation of very near-primary $\delta^{13}C$ signatures in the investigated Upper Cambrian lime mudstone beds (rhythmites) of the continuous lower section at Martin Point in western Newfoundland. The $\delta^{13}C$ profile shows two main negative excursions, a lower excursion (~4 ‰) that can be correlated with the global SPICE event (*Proconodontus posterocostatus* Zone) and an upper post-SPICE one (~6 ‰) that can be correlated with the *Proconodontus muelleri* conodont Zone. However, the *muelleri* and the underlying *posterocostatus* zones, or possibly their equivalents, have not yet been documented in the Martin Point section, and the chemostratigraphic correlation has to therefore be taken with caution.

(b) The SPICE and post-SPICE negative $\delta^{13}C$ excursions provide a potential tool for the global correlation of the Upper Cambrian in eastern Laurentia with equivalent sections on the same palaeocontinent and beyond.

(c) The lack of sedimentary hiatuses and retention of a primary $\delta^{13}C$ profile, with distinct excursions recording the global events from the early Late Cambrian to the Є–O boundary, make the succession at Martin Point a potential complete Upper Cambrian reference section on Laurentia.

Acknowledgements. The author wishes to thank two anonymous reviewers for their constructive reviews. Also, the efforts of Chad Deering (editor) are much appreciated. Special thanks to Dr. Svend Stouge for his help with the fieldwork. This project was supported by funding (to Karem Azmy) from the Petroleum Exploration Enhancement Program (PEEP), NL, Canada.

References

Azmy K (2018) Carbon-isotope stratigraphy of the uppermost Cambrian in eastern Laurentia: implications for global correlation. *Geological Magazine*, published online 12 February 2018. doi: 10.1017/S001675681800002X.

Azmy K, Kendall K, Brand U, Stouge S and Gordon GW (2015) Redox conditions across the Cambrian–Ordovician boundary: elemental and isotopic signatures retained in the GSSP carbonates. *Palaeogeography, Palaeoclimatology, Palaeoecology* **440**, 440–54.

Azmy K, Stouge S, Brand U, Bagnoli G and Ripperdan R (2014) High-resolution chemostratigraphy of the Cambrian–Ordovician GSSP in western Newfoundland, Canada: enhanced global correlation tool. *Palaeogeography, Palaeoclimatology, Palaeoecology* **409**, 135–44.

Azmy K, Stouge S, Christiansen JL, Harper DAT, Knight I and Boyce D (2010) Carbon-isotope stratigraphy of the Lower Ordovician succession in Northeast Greenland: implications for correlations with St. George Group in western Newfoundland (Canada) and beyond. *Sedimentary Geology* **225**, 67–81.

Azomani E, Azmy K, Blamey N, Brand U and Al-Aasm I (2013) Origin of lower Ordovician dolomites in eastern Laurentia: controls on porosity and implications from geochemistry. *Marine and Petroleum Geology* **40**, 99–114.

Bahamonde JR, Merino-Tomé OA and Heredis N (2007) A Pennsylvanian microbial boundstone-dominated carbonate shelf in a distal foreland margin (Picos de Europa Province, NW Spain). *Sedimentary Geology* **198**, 167–93.

Barnes CR (1988) The proposed Cambrian–Ordovician global boundary stratotype and point (GSSP) in western Newfoundland, Canada. *Geological Magazine* **125**, 381–414.

Bartley JK, Kah LC, Frank TD and Lyons TW (2015) Deep-water microbialites of the Mesoproterozoic Dismal Lakes Group: microbial growth, lithification, and implications for coniform stromatolites. *Geobiology* **13**, 15–32.

Brand U, Logan A, Bitner MA, Griesshaber E, Azmy K and Buhl D (2011) What is the ideal proxy of Paleozoic seawater chemistry? *Memoirs of the Association of Australasian Palaeontologists* **41**, 9–24.

Brasier MD (1993) Towards a carbon isotope stratigraphy of Cambrian System: potential of the Great Basin succession. In *High Resolution Stratigraphy* (eds EA Hailwood and RB Kidd), pp. 341–50. Geological Society of London, Special Publication no. 70.

Buggisch W, Keller M and Lehnert O (2003) Carbon isotope record of Late Cambrian to early Ordovician carbonates of the Argentine Precordillera. *Palaeogeography, Palaeoclimatology, Palaeoecology* **195**, 357–73.

Cawood PA, McCausland PJA and Dunning GR (2001) Opening Iapetus: constraints from Laurentian margin in Newfoundland. *Geological Society of America Bulletin* **113**, 443–53.

Coniglio M and James NP (1990) Origin of fine-grained carbonate and siliciclastic sediments in an Early Paleozoic slope sequence, Cow Head Group, Western Newfoundland. *Sedimentology* **37**, 215–30.

Cooper RA, Nowlan GS and Williams SH (2001) Global stratotype section and point for base of the Ordovician system. *Episodes* **24**, 19–28.

Dahl TW, Boyle RA, Canfield DE, Connelly JN, Gill BC, Lenton TM and Bizzaro M (2014) Uranium isotopes distinguish two geochemically distinct stages during the later Cambrian SPICE event. *Earth and Planetary Science Letters* **401**, 313–26.

Della Porta G, Kenter JAM, Bahamonde JR, Immenhauser A and Villa E (2003) Microbial boundstone dominated carbonate slopes (Upper Carboniferous, N. Spain): microfacies, lithofacies distribution and stratal geometry. *Facies* **49**, 175–207.

Dickson JAD (1966) Carbonate identification and genesis as revealed by staining. *Journal of Sedimentary Petrology* **36**, 491–505.

Fan R, Deng SH and Zhang XL (2011) Significant carbon isotope excursions in the Cambrian and their implications for global correlations. *Science China Earth Sciences* **54**, 1686–95.

Gill BC, Lyons TW, Young SA, Kump LR, Knoll AH and Saltzman MR (2011) Geochemical evidence for widespread euxinia in the later Cambrian ocean. *Nature* **469**, 80–3.

Glumac B and Mutti LE (2007) Late Cambrian (Steptoean) sedimentation and responses to seal-level change along the northeastern Laurentian margin: insights from carbon isotope stratigraphy. *Geological Society of America Bulletin* **119**, 623–36.

Halverson GP, Hoffman PF, Schrag DP, Maloof AC and Rice AHN (2005) Toward a Neoproterozoic composite carbon-isotope record. *Geological Society of America Bulletin* **117**, 1181–207.

Hibbard JP, Van Staal CR and Rankin DW (2007) A comparative analysis of pre-Silurian crustal building blocks of the northern and southern Appalachian Orogen. *American Journal of Science* **307**, 23–45.

Hurtgen MT, Pruss SB and Knoll AH (2009) Evaluating the relationship between the carbon and sulfur cycles in the later Cambrian ocean: an example from the Port au Port Group, western Newfoundland, Canada. *Earth and Planetary Science Letters* **281**, 288–97.

James NP and Stevens PK (1986) Stratigraphy and correlation of the Cambro–Ordovician Cow Head Group, western Newfoundland. *Geological Survey of Canada Bulletin* **366**, 1–143.

James NP, Stevens RK, Barnes CR and Knight I (1989) Evolution of a Lower Paleozoic continental-margin carbonate platform, northern Canadian Appalachians. In *Controls on Carbonate Platform and Basin Development* (eds PD Crevello, JL Wilson, JF Sarg and JF Read), pp. 123–46. Society of Economic Paleontologists and Mineralogists, Special Publication no. 44.

Jing X-C, Deng S-H, Zhao Z-J, Lu Y-Z and Zhang S-B (2008) Carbon isotope composition and correlation across the Cambrian–Ordovician boundary in Kalpin Region of the Tarim Basin, China. *Science in China: Earth Sciences* **51**, 1317–59.

Landing E (2007) Ediacaran–Ordovician of east Laurentia——geologic setting and controls on deposition along the New York Promontory. In *S. W. Ford Memorial Volume: Ediacaran–Ordovician of East Laurentia* (ed. E Landing), pp. 5–24. New York State Museum Bulletin no. 510.

Landing E (2012a) Time-specific black mudstones and global hyperwarming on the Cambrian–Ordovician slope and shelf of the Laurentia palaeocontinent. *Palaeogeography, Palaeoclimatology, Palaeoecology* **367–368**, 256–72.

Landing E (2012b) The Great American Carbonate Bank in Eastern Laurentia: its births, deaths, and linkage to paleooceanic oxygenation (Early Cambrian–Late Ordovician). In *The Great American Carbonate Bank: The Geology and Economic Resources of the Cambrian–Ordovician Sauk Megasequence of Laurentia* (eds JR Derby, RD Fritz, SA Longacre, WA Morgan and CA Sternbach), pp. 451–92. American Association of Petroleum Geologists Memoir 98.

Landing E, Westrop SR and Adrain JM (2011) The Lawsonian Stage – the Eoconodontus notchpeakensis FAD and HERB carbon isotope excursion define a globally correlatable terminal Cambrian stage. *Bulletin of Geosciences* **86**, 621–40.

Landing E, Westrop SR and Miller JF (2010) Globally practical base for the uppermost Cambrian (Stage 10): FAD of the conodont Eoconodontus notchpeakensis and the Housian [sic, read 'Lawsonian' as the abstract text] Stage. In *The 15th Field Conference of the Cambrian Stage Subdivision Working Group. Abstracts and Excursion Guide, Prague, Czech Republic and South-eastern Germany* (eds O Fatka and P Budil), p. 18. Prague: Czech Geological Survey.

Lavoie D, Desrochers A, Dix G, Knight I and Hersi OS (2012) The Great Carbonate Bank in eastern Canada: an overview. In *The Great American Carbonate Bank: The Geology and Economic Resources of Cambrian–Ordovician Sauk Megasequence of Laurentia* (eds JR Derby, RD Fritz, SA Longacre, WA Morgan and CA Sternbach), pp. 499–524. American Association of Petroleum Geologists, Memoir 98.

Lazarenko NP, Gogin IY, Pegel TV and Abaimova GP (2011) The Khos-Nelege River section of the Ogon'or Formation: a potential candidate for the GSSP of Stage 10, Cambrian System. *Bulletin of Geosciences* **86**, 555–68.

Li X, Jenkyns HC, Wang C, Hu X, Chen X, Wei Y, Huang Y and Cui J (2006) Upper Cretaceous carbon- and oxygen-isotope stratigraphy of hemipelagic carbonate facies from southern Tibet, China. *Journal of the Geological Society, London* **163**, 375–82.

Li D, Zhang X, Chen K, Zhang G, Chen X, Huang W, Peng S and Shen Y (2017) High-resolution C-isotope chemostratigraphy of the uppermost Cambrian stage (Stage 10) in South China: implications for defining the base of Stage 10 and palaeoenvironmental change. *Geological Magazine* **154**, 1232–43.

Machel HG and Burton EA (1991) Factors governing cathodoluminescence in calcite and dolomite, and their implications for studies of carbonate diagenesis. In *Luminescence Microscopy and Spectroscopy: Qualitative and Quantitative Applications. SEPM Short Course Notes, No. 25* (eds CE Barker, RC Burruss, OC Kopp, HG Machel, DJ Marshall, P Wright and HY Colbum), pp. 37–57. Tulsa, OK: SEPM Society for Sedimentary Geology.

Miller JF, Evans KR, Ethington RL, Freeman RL, Loch JD, Popov LE, Repetski JE, Ripperdan RL and Taylor JF (2015) Proposed Auxiliary Boundary Stratigraphic Section and Point (ASSP) for the base of the Ordovician System at Lawson Cove, Utah, USA. *Stratigraphy* **12**, 219–36.

Miller JF, Evans KR, Freeman RL, Ripperdan RL and Taylor JF (2011) Proposed stratotype for the base of the Lawsonian Stage (Cambrian Stage 10) at the first appearance datum of Eoconodontus notchpeakensis (Miller) in the House Range, Utah, USA. *Bulletin of Geosciences* **86**, 595–620.

Miller JF, Repetski JE, Nicoll RS, Nowlan G and Ethington RL (2014) The conodont Iapetognathus and its value for defining the base of the Ordovician system. *GFF* **136**, 185–8.

Peng S, Babcock LE and Cooper RA (2012) The Cambrian period. In *The Geologic Time Scale 2012* (eds FM Gradstein, JG Ogg, M Schmitz and G Ogg), pp. 437–88. Oxford, UK: Elsevier.

Ripperdan RL, Magaritz M, Nicoll RS and Shergold JH (1992) Simultaneous changes in carbon isotopes, sea level, and conodont biozones within the Cambrian–Ordovician boundary interval at Black Mountain, Australia. *Geology* **20**, 1039–41.

Rush PF and Chafetz HS (1990) Fabric retentive, non-luminescent brachiopods as indicators of original $\delta^{13}C$ and $\delta^{18}O$ compositions: a test. *Journal of Sedimentary Petrology* **60**, 968–81.

Saltzman MR, Cowan CA, Runke AC, Runnegar B, Stewart MC and Palmer AR (2004) The late Cambrian SPICE (δ13C) event and the Sauk II–Sauk III regression: new evidence from Laurentian basins in Utah, Iowa, and Newfoundland. *Journal of Sedimentary Research* **74**, 366–77.

Saltzman MR, Ripperdan RL, Brasier MD, Ergaliev GK, Lohmann KC, Robison RA, Chang WT, Peng S and Runnegar B (2000) A global carbon isotope excursion during the Late Cambrian: relation to trilobite extinctions, organic matter burial and sea level. *Palaeogeography, Palaeoceanography, Palaeoclimatology* **162**, 211–23.

Schmid S (2011) Chemostratigraphy and palaeo-environmental characterisation of the Cambrian stratigraphy in the Amadeus Basin, Australia. *Chemical Geology* **451**, 169–82.

Sial AN, Peralta S, Gaucher C, Alonso RN and Pimentel MA (2008) Upper Cambrian carbonate sequences of the Argentine Precordillera and the Steptoean C-Isotope Positive Excursion (SPICE). *Gondwana Research* **13**, 437–52.

Sial AN, Peralta S, Gaucher C, Toselli AJ, Ferreira VP, Frei R, Parada MA, Pimentel MM and Pereira NS (2013) High-resolution stable isotope stratigraphy of the upper Cambrian and Ordovician in the Argentine Precordillera: carbon isotope excursions and correlations. *Gondwana Research* **24**, 330–48.

Terfelt F, Eriksson ME and Schmitz B (2014) The Cambrian–Ordovician transition in dysoxic facies in Baltica – diverse faunas and carbon isotope anomalies. *Palaeogeography, Palaeoclimatology, Palaeoecology* **394**, 59–73.

Veizer J (1983) Chemical diagenesis of carbonates. In *Theory and Application of Trace Element Technique, Stable Isotopes in Sedimentary Geology. SEPM Short Course Notes, No. 10* (eds MA Arthur, TF Anderson, IR Kaplan, J Veizer and LS Land), pp. 3-1–3-100. Tulsa, OK: SEPM Society for Sedimentary Geology.

Veizer J, Ala D, Azmy K, Bruckschen P, Bruhn F, Buhl D, Carden G, Diener A, Ebneth S, Goddris Y, Jasper T, Korte C, Pawellek F, Podlaha O and Strauss H (1999). $^{87}Sr/^{86}Sr$, $\delta^{18}O$ and $\delta^{13}C$ evolution of Phanerozoic seawater. *Chemical Geology* **161**, 59–88.

Westrop SR, Adrain JM and Landing E (2011) The Cambrian (Sunwaptan, Furongian) agnostoid arthropod Lotagnostus Whitehouse, 1936, in Laurentian and Avalonian North America: systematics and biostratigraphic significance. *Bulletin of Geosciences, Czech Geological Survey* **86**, 569–94.

Wilson JL, Medlock PL, Fritz RD, Canter KL and Geesaman RG (1992) A review of Cambro-Ordovician breccias in North America. In *Paleokarst, Karst-Related Diagenesis, and Reservoir Development: Examples from Ordovician–Devonian Age Strata of West Texas and the Mid-Continent: 1* (eds MP Candelaria and CL Reed), pp. 19–29. Tulsa, OK: SEPM–Permian Basin Section, Publication 92–33.

Woods MA, Wilby PR, Leng MJ, Rushton AWA and Williams M (2011) The Furongian (late Cambrian) Steptoean Positive Carbon Isotope Excursion (SPICE) in Avalonia. *Journal of the Geological Society, London* **168**, 851–61.

Appendix

Table A1. Elemental and isotopic geochemical compositions of the lower section of the Martin Point carbonates

Sample id no.	$\delta^{13}C$ ‰VPDB	$\delta^{18}O$ ‰VPDB	$CaCO_3$ %	$MgCO_3$ %	Sr (ppm)	Mn (ppm)	Fe (ppm)	Al (ppm)
B1-3	−1.68	−7.33	96.5	3.5	202	545	5017	555
B2-1	−3.85	−7.67	96.4	3.6	195	511	4018	491
B2-1R	−4.26	−7.89						
B2-2	−2.28	−7.09						
B4-1	−2.40	−7.12	99.2	0.8	175	334	755	186
B6	−1.30	−7.58	93.0	7.0	282	367	5770	1655
B8	−0.67	−6.02	70.2	29.8	73	266	7007	783
B10	−0.58	−7.38	99.0	1.0	161	248	590	568
B12	−1.38	−7.48	98.6	1.4	181	335	851	238
B14-1	−0.96	−8.11						
B14-2	−0.02	−7.58	98.8	1.2	360	196	724	181
B14-3	−0.67	−7.41						
B16-1	−0.41	−7.55						
B16-3	−0.32	−7.93						
B18-1	−0.74	−8.15	99.4	0.6	121	333	783	114
B19	−0.76	−7.97	98.6	1.4	195	266	1372	249
B20-2	−0.48	−7.16	99.0	1.0	226	165	782	301
B22-1	−0.42	−7.30	99.3	0.7	252	221	482	171
B22-3	−1.06	−8.24						
B22-5	−1.51	−7.71	92.9	7.1	146	280	4798	475
B23-2	−0.94	−6.94	99.0	1.0	160	317	977	432
B23-3	−1.31	−7.57						
B23-6	−1.32	−7.52						
B23-9	−0.39	−7.53	99.4	0.6	1294	103	487	134
B27-1	−0.59	−7.59						
B29-3	0.30	−7.30	98.2	1.8	590	91	1185	618
B29-5	−0.07	−7.60						
B29-7	−0.79	−7.00	98.9	1.1	173	176	816	585
B31-2	−0.11	−7.91						
B31-3	0.27	−8.17						
B31-4	0.70	−6.96	98.6	1.4	275	256	1137	566
B31-7	0.01	−7.03						
B31-9	0.68	−7.17						
B31-11	−0.38	−7.34	99.0	1.0	206	128	608	832
B32	−0.69	−5.28						
B33-2	0.96	−6.74	98.7	1.3	290	179	397	207
B35-1	−0.88	−7.01	98.7	1.3	259	172	501	81
B35-3	−1.40	−7.14	98.7	1.3	336	257	948	124
B36a-2	−4.79	−7.46	98.6	1.4	212		792	281
B36a-3	−0.80	−7.55	98.8	1.2	205	605	1778	517
B36a-4	−1.29	−7.60						
B36a-5	−3.92	−7.63	98.8	1.2	189	802	1160	674
B36a-6	−2.66	−7.31	98.7	1.3	243			487
B36c-1	−0.12	−7.39	97.3	2.7	387	322	2627	620

https://doi.org/10.1017/S0016756818000638 Published online by Cambridge University Press

Table A1. Continued

Sample id no.	$\delta^{13}C$ ‰VPDB	$\delta^{18}O$ ‰VPDB	$CaCO_3$ %	$MgCO_3$ %	Sr (ppm)	Mn (ppm)	Fe (ppm)	Al (ppm)
B36c-2	0.56	−7.40	98.9	1.1	547	301	1262	387
B36c-3	0.32	−7.68						
B36c-4	−1.96	−7.27	97.6	2.4	561	202	1241	316
B36d-1	−0.72	−6.99	98.8	1.2	436	183	455	357
B36d-2	−1.04	−7.33	98.9	1.1	504	339	822	274
B36e	−0.40	−7.61	98.5	1.5	404	240	2093	542

https://doi.org/10.1017/S0016756818000638 Published online by Cambridge University Press